Sensor-based Simultaneous Localization and Mapping – Part I: GAS Robocentric Filter

Bruno J. Guerreiro, Pedro Batista, Carlos Silvestre, and Paulo Oliveira

Abstract— This paper presents the design, analysis, and experimental validation of a sensor-based globally asymptotically stable (GAS) filter for simultaneous localization and mapping (SLAM) with application to uninhabited aerial vehicles (UAVs). The SLAM problem is first formulated in a sensor-based framework, without any type of vehicle pose information, and modified in such a way that the underlying system structure can be regarded as linear time varying for observability, filter design, and convergence analysis purposes. Thus, a Kalman filter follows naturally with GAS error dynamics that estimates, in a robocentric coordinate frame, the positions of the landmarks, the velocity of the vehicle, and the bias of the angular velocity measurement. The online inertial map and trajectory estimation is detailed in a companion paper and follows from the estimation solution provided by the SLAM filter herein presented. The performance and consistency of the proposed method are successfully validated experimentally in a structured real world environment using a quadrotor instrumented platform.

I. INTRODUCTION

Reliable navigation and positioning of uninhabited aerial vehicles (UAV) are fundamental for any autonomous mission, particularly in unknown environments where absolute positioning systems are absent or unreliable. The motivation for this work arises from the usage of autonomous rotorcraft for automatic inspection of critical infrastructures and buildings, such as bridges, electric power lines, dams, construction areas, etc. Near these structures, the ubiquitous global positioning system (GPS) signal may be unreliable or completely unavailable, whereas the electromagnetic interference may degrade any magnetometer measurement to the point of becoming unusable. Therefore, aided navigation strategies have to be devised in such a way that these sensors are made redundant.

This paper presents a globally asymptotically stable (GAS) sensor-based filter for simultaneous localization and mapping (SLAM) with application to uninhabited aerial vehicles (UAVs) in GPS-denied environments, using acceleration and angular rate inertial measurements, a LASER scanning device and an altitude sensor. Over the past decades the research community has devoted tremendous effort in the field of probabilistic SLAM. The seminal works that established the statistical foundations for describing the relationships between landmarks and their correlations include [1], and [2]. For a detailed survey and tutorial on SLAM please refer to [3], [4], and references therein, which include a significant number of successful implementations of SLAM algorithms in real world scenarios. A general proof of global convergence for the extended Kalman filter (EKF), to the best of the authors' knowledge, is yet to be found. Nonetheless, there are some notable EKF-based SLAM convergence results [5], [6], which usually assume that the linearized system matrices are evaluated at the ideal values of the state variables. This linearization may lead to statistical inconsistency as it was first pointed out in [7] and subsequently acknowledged and discussed in [8] and [9]. In order to minimize the inconsistency problems induced by the linearization, some new algorithms have been proposed, such as the robocentric map joining algorithm [10], where the filtering is made in the sensor space, or the first-estimates Jacobian EKF [11].

The main contribution of this paper is the design, analysis, and experimental validation of a novel sensor-based SLAM filter for structured 3-dimensional (3-D) environments, 2-D mapping and altitude, as part of an integrated SLAM algorithm, that: (i) has globally asymptotically stable error dynamics; (ii) allows for online simultaneous estimation of the inertial frame map, position and motion of the vehicle, as detailed in the companion paper [12]; (iii) resorts to the linear and angular motion kinematics, which are exact; (iv) can easily be generalized into full 3-D SLAM, if 3-D landmarks are available; (v) builds on the well-established linear time-varying (LTV) Kalman filtering theory; and (vi) estimates explicitly the rate gyro bias, merging low bandwidth landmark observations with high bandwidth rate gyro measurements. The result of this filter is the solution of the SLAM problem in the vehicle frame, where the vehicle pose is deterministic, as it corresponds to that of the vehicle frame, and the positions of the landmarks rotate and translate according to the vehicle motion, in a similar fashion to what happens in [10]. An essential feature of the filter design is the modification of the nominal nonlinear sensor-based system dynamics such that it can be regarded as LTV for observability and convergence analysis purposes, even though it still is intrinsically nonlinear. Nevertheless, it must be stressed that the resulting system dynamics used in the design and analysis of the Kalman filter are exact and no approximations or linearizations are performed whatsoever. The proposed solution builds on previous sensor-based navigation filters

B. J. Guerreiro, P. Batista, C. Silvestre, and Paulo Oliveira are with the Institute for Systems and Robotics, Instituto Superior Técnico, at the Technical University of Lisbon, Av. Rovisco Pais 1, 1049-001 Lisboa, Portugal. C. Silvestre is also with the Faculty of Science and Technology, University of Macau, Taipa, Macau.
{bguerreiro,pbatista,cjs,pjcro}@isr.ist.utl.pt

proposed by the authors in [13], [14], and [15].

The second part of the proposed SLAM algorithm, which is detailed in the companion paper [12], focus on the online optimal transformation of the estimated sensor-based map into the inertial frame, by estimating the translation and rotation between any two consecutive instants, provided at least two landmark associations.

The paper is organized as follows. Section II introduces the sensor-based paradigm, the nominal system dynamics, and the problem at hand. A constructive observability analysis is presented in Section III and Section IV details the definition of the SLAM filter. Experimental results using an instrumented quadrotor platform are shown and discussed in Section V and, finally, in Section VI, some concluding remarks and directions of future work are provided.

Throughout the paper the symbol $\mathbf{0}_{n \times m}$ denotes an $n \times m$ matrix of zeros, $\mathbf{I}_n$ an identity matrix with dimension $n \times n$, and $\mathrm{diag}(\mathbf{A}_1, \ldots, \mathbf{A}_n)$ a block diagonal matrix. When the dimensions are omitted the matrices are assumed of appropriate dimensions.

II. PROBLEM STATEMENT

A. Sensor-based framework

The traditional EKF-based SLAM filter represents the estimated features and vehicle pose using an absolute reference frame, usually denoted inertial frame, while the measurements are obtained in body-fixed coordinates, i.e., in the frame rigidly attached to the vehicle. The core concept of the sensor-based SLAM approach that is presented in this paper is to design the filter directly in the space of the sensors, avoiding any representation of the attitude of the vehicle and taking into account the original noise characteristics of each sensor. Note also that, for control purposes, it is usually the quantities in the robocentric frame that are required, with the so-called sensor-based control paradigm, and that the proposed filter readily estimates.

B. Definition of frames and sensor measurements

Let $\{I\}$ denote the local inertial frame, $\{B\}$ the body-fixed frame, and $_B^I \mathbf{R}(t) \in \mathrm{SO}(3)$ the rotation matrix from $\{B\}$ to $\{I\}$. Let also $^I\mathbf{p}_B(t) \in \mathbb{R}^3$ denote the position of the origin of $\{B\}$, described in $\{I\}$, and $\mathbf{v}_B(t) \in \mathbb{R}^3$ the velocity of the vehicle relative to $\{I\}$, expressed in $\{B\}$. The linear motion kinematics of the vehicle is given by $^I\dot{\mathbf{p}}_B(t) = {}_B^I\mathbf{R}(t)\mathbf{v}_B(t)$, while the angular motion kinematics satisfy $_B^I\dot{\mathbf{R}}(t) = {}_B^I\mathbf{R}(t)\mathbf{S}[\boldsymbol{\omega}_B(t)]$, where $\boldsymbol{\omega}_B(t) \in \mathbb{R}^3$ is the angular velocity of the vehicle, expressed in $\{B\}$, and $\mathbf{S}[\boldsymbol{\omega}_B(t)]$ is the skew-symmetric matrix such that $\mathbf{S}[\boldsymbol{\omega}_B(t)]\mathbf{d}(t)$ is the cross product $\boldsymbol{\omega}_B(t) \times \mathbf{d}(t)$, for some $\mathbf{d}(t) \in \mathbb{R}^3$. Consider also the ZYX-Euler angles which can be used to decompose the rotation matrix $_B^I\mathbf{R}(t)$ as $_B^I\mathbf{R}(t) = \mathbf{R}_z(\psi(t))\,\mathbf{R}_y(\theta(t))\,\mathbf{R}_x(\phi(t))$, where $\psi(t)$, $\theta(t)$, and $\phi(t)$ denote the yaw, pitch, and roll angles, respectively. Using standard filtering techniques (see for instance [16] and references therein), the roll and pitch angles can be obtained using only rate gyros and accelerometer measurements, enabling the definition of an horizontal body-fixed frame $\{H\}$, such that $^I\mathbf{p}_H(t) = {}^I\mathbf{p}_B(t)$,

$_H^I\mathbf{R}(t) = \mathbf{R}_z(\psi(t))$, and $_B^H\mathbf{R}(t) = \mathbf{R}_y(\theta(t))\,\mathbf{R}_x(\phi(t))$. Using known transformations, the measurements provided by laser scanning sensors can be transformed into $\{B\}$, and using $_B^H\mathbf{R}(t)$ they can be projected and seen as sensors in $\{H\}$. Considering a LASER scanner mounted horizontally in the vehicle, so that the measurements in $\{H\}$ represent a projected horizontal profile of the environment, and an altitude sensor, either a sonar or a LASER range finder, the complete 3-dimensional (3-D) position and a 2-dimensional (2-D) map of the environment can be obtained using a simultaneous localization and mapping (SLAM) algorithm. The underlying standard assumption is that the environment is fairly structured in the vertical direction.

Consider that each detected landmark can be represented by a 2-D position and some auxiliary characteristics depending on the type of feature. For the sake of clarity, the remainder of this paper considers only the 2-D position of each landmark, and with a slight abuse of notation, all vectors are in 2-D and all rotation matrices belong to SO(2), unless otherwise stated. The position of the i-th landmark in $\{H\}$ is denoted by $\mathbf{p}_i(t) \in \mathbb{R}^2$ and satisfies

$$\mathbf{p}_i(t) = {}_H^I\mathbf{R}^T(t)\,[^I\mathbf{p}_i - {}^I\mathbf{p}_H(t)]$$

where $^I\mathbf{p}_i \in \mathbb{R}^2$ denotes the inertial 2-D position of the landmark. In the sensor-based framework, the kinematics of this landmark can be written as

$$\dot{\mathbf{p}}_i(t) = -\,[r_m(t) - b_r(t)]\,\mathbf{S}\,\mathbf{p}_i(t) - \mathbf{v}(t)$$

where $\mathbf{S} = \begin{bmatrix} 0 & -1 \\ 1 & 0 \end{bmatrix} \in \mathbb{R}^{2\times 2}$, $r_m(t) \in \mathbb{R}$ is the z-component of rate gyro measurements expressed in $\{H\}$, $b_r(t) \in \mathbb{R}$ is the corresponding rate gyro bias, and $\mathbf{v}(t) \in \mathbb{R}^2$ denotes the velocity of the vehicle relative to the inertial frame, expressed in $\{H\}$. Notice that, because the bias term is expressed in $\{H\}$, it is not really constant. Instead, its derivative depends on the roll, pitch, and respective angular velocities, which can all be obtained using a complementary filter with globally asymptotically stable based on the acceleration and rate gyro readings, see [16] for details. In the remainder of the paper it is considered, with no loss of generality for observer design purposes, $\dot{b}_r(t) = 0$. In the final design the additional input is naturally considered.

C. Problem Statement

In every SLAM state-space formulation, the full stochastic state vector, here denoted as $\mathbf{x}_F \in \mathbb{R}^{n_{x_F}}$, can be decomposed into vehicle specific variables, $\mathbf{x}_V \in \mathbb{R}^{n_{x_v}}$, and landmark variables, $\mathbf{x}_M \in \mathbb{R}^{n_{x_M}}$. In the proposed formulation, the vehicle state vector is formed by the altitude $z(t) \in \mathbb{R}$, the linear velocity in $\{H\}$, $\mathbf{v}(t) \in \mathbb{R}^2$, the vertical velocity $v_z(t) \in \mathbb{R}$, and the bias of the angular velocity in $\{H\}$, $b_r(t) \in \mathbb{R}$, yielding $\mathbf{x}_V(t) = \begin{bmatrix} z(t) & \mathbf{v}(t) & v_z(t) & b_r(t) \end{bmatrix}^T$. A further decomposition of the landmark state into observed and unobserved landmarks is considered, for the sake of clarity, such that $\mathbf{x}_M = \begin{bmatrix} \mathbf{x}_{MO}^T & \mathbf{x}_{MU}^T \end{bmatrix}^T$, where $\mathbf{x}_{MO} = \{\mathbf{p}_i\} \in \mathbb{R}^{n_{x_m}}$, for all $i \in \mathcal{I}_O$, with $\mathcal{I}_O = \{o_1, \ldots, o_{no}\}$, and $\mathbf{x}_{MU} = \{\mathbf{p}_i\} \in \mathbb{R}^{n_{x_{MU}}}$, for all $i \in \mathcal{I}_U$. Note that the union of

the sets of observed and unobserved landmarks, respectively, $\mathcal{I}_O$ and $\mathcal{I}_U$, yields $\mathcal{I} = \mathcal{I}_O \cup \mathcal{I}_U = \{1, \dots, n_M\}$. With the above introduction and considering that the linear velocities are slowly time-varying, the complete system dynamics in $\{H\}$ can now be written as

$$\begin{cases} \dot{\mathbf{x}}_V(t) = \mathbf{A}_V \, \mathbf{x}_V(t) \\ \dot{\mathbf{p}}_i(t) = \mathbf{A}_{MV_i}(\mathbf{p}_i(t)) \, \mathbf{x}_V(t) + \mathbf{A}_{M_i}(t) \, \mathbf{p}_i(t) \; \forall_{i \in \mathcal{I}} \\ y_z(t) = \mathbf{C}_z \, \mathbf{x}_V(t) \\ \mathbf{y}_{MO}(t) = \mathbf{x}_{MO}(t) \end{cases}, \quad (1)$$

where it is a matter of algebraic manipulation to obtain

$$\mathbf{A}_V = \begin{bmatrix} 0 & \mathbf{0}_{1 \times 2} & -1 & 0 \\ \mathbf{0}_{2 \times 1} & \mathbf{0}_{2 \times 2} & \mathbf{0}_{2 \times 1} & \mathbf{0}_{2 \times 1} \\ 0 & \mathbf{0}_{1 \times 2} & 0 & 0 \\ 0 & \mathbf{0}_{1 \times 2} & 0 & 0 \end{bmatrix},$$

$$\mathbf{A}_{MV_i}(\mathbf{p}_i(t)) = \begin{bmatrix} \mathbf{0}_{2 \times 1} & -\mathbf{I}_2 & \mathbf{0}_{2 \times 1} & \mathbf{S}\,\mathbf{p}_i(t) \end{bmatrix},$$

with $\mathbf{A}_{M_i}(t) = -r_m(t) \, \mathbf{S}$ and $\mathbf{C}_z = \begin{bmatrix} 1 & \mathbf{0}_{1 \times 2} & 0 & 0 \end{bmatrix}$.

The problem considered in this paper is that of designing a filter with globally asymptotically stable error dynamics for the nominal nonlinear system (1), considering additive system disturbances and sensor noise. Note that the position of the vehicle and its orientation, as well as the position of each landmark in frame $\{I\}$, can be computed online as a solution of a classical optimization problem with closed-form solution, as it is shown in the companion paper [12].

III. OBSERVABILITY ANALYSIS

In this section the observability of the nonlinear system (1) is analyzed. In a SLAM filter the observed/visible landmarks are a subset of the state landmarks, and the unobserved/non-visible landmarks are integrated in open-loop. The main focus of this section is to prove that this formulation of the SLAM problem, where the unobserved landmarks are not considered for observability purposes, is observable. In addition, the analysis is constructive in the sense that a Kalman filter can be readily applied, identifying the non-linear system with a particular linear time-varying system, yielding globally asymptotically stable error dynamics, as successfully applied in the past by the authors [14].

Discarding the unobserved landmarks, the reduced state vector is $\mathbf{x}(t) = \begin{bmatrix} \mathbf{x}_V^T(t) & \mathbf{x}_{MO}^T(t) \end{bmatrix}^T \in \mathbb{R}^{n_x}$, while the output vector is $\mathbf{y}(t) = \begin{bmatrix} y_z(t) & \mathbf{y}_{MO}^T(t) \end{bmatrix}^T \in \mathbb{R}^{n_y}$. Thus, it is straightforward to rewrite (1) as

$$\begin{cases} \dot{\mathbf{x}}(t) = \mathbf{A}(t)\,\mathbf{x}(t) \\ \mathbf{y}(t) = \mathbf{C}\,\mathbf{x}(t) \end{cases}, \quad (2)$$

where

$$\mathbf{A}(t) = \begin{bmatrix} \mathbf{A}_v & \mathbf{0}_{n_{x_v} \times n_{x_m}} \\ \mathbf{A}_{MV}(t) & \mathbf{A}_M(t) \end{bmatrix} \in \mathbb{R}^{(n_{x_v} + n_{x_m}) \times (n_{x_v} + n_{x_m})},$$

$$\mathbf{A}_{MV}(t) = \begin{bmatrix} \mathbf{A}_{MV_{o_1}}^T(t) & \dots & \mathbf{A}_{MV_{o_{no}}}^T(t) \end{bmatrix}^T \in \mathbb{R}^{n_{x_m} \times n_{x_v}},$$

$$\mathbf{A}_{MV_i}(t) = \mathbf{A}_{MV_i}(\mathbf{p}_{i_m}(t)) \; \forall_{i \in \mathcal{I}_O},$$

$$\mathbf{A}_M(t) = \mathrm{diag}\left(\mathbf{A}_{M_{o_1}}(t), \dots, \mathbf{A}_{M_{o_{no}}}(t) \right) \in \mathbb{R}^{n_{x_m} \times n_{x_m}},$$

and

$$\mathbf{C} = \begin{bmatrix} \mathbf{C}_z & \mathbf{0}_{1 \times n_{x_m}} \\ \mathbf{0}_{n_{x_m} \times n_{x_v}} & \mathbf{I}_{n_{x_m}} \end{bmatrix} \in \mathbb{R}^{(1 + n_{x_m}) \times (n_{x_v} + n_{x_m})},$$

where the subscript $_m$ denotes a measured variable. Notice that the dynamic system (2) can be regarded as a LTV system, even though it still is, in fact, a nonlinear system. This is so because the system matrix $\mathbf{A}(t)$ depends on the system output, i.e., $\mathbf{A}(t) = \mathbf{A}(t, \mathbf{y}(t))$. However, this is not a problem for observability analysis and observer design purposes, as the output $\mathbf{y}(t)$ is available and can simply be considered as a known function of t, see [14, Lemma 1].

The following theorem establishes a sufficient condition for observability of the nonlinear system (2).

Theorem 1: Let $\mathcal{T} := [t_0, t_f]$. If there exists a time instant $t_i \in \mathcal{T}$ such that there exist at least two observed landmarks for $t = t_i$ or, equivalently, there exist two landmarks $\mathbf{p}_{o_{1_m}}(t_i)$ and $\mathbf{p}_{o_{2_m}}(t_i)$ such that, $\mathbf{p}_{o_{1_m}}(t_i) \neq \mathbf{p}_{o_{2_m}}(t_i)$, then the system (2) is observable on $\mathcal{T}$ in the sense that, given the system output, the initial condition is uniquely defined.

Proof: Using Lemma [14, Lemma 1], the nonlinear system (2) is observable on $\mathcal{T}$ if the observability Gramian associated with the pair $(\mathbf{A}(t), \mathbf{C}(t))$ on $\mathcal{T}$ is invertible. The proof follows by establishing that this is the case. In order to simplify the analysis, let $\mathbf{R}_m(t) \in SO(2)$ be a rotation matrix such that $\dot{\mathbf{R}}_m(t) = r_m(t)\mathbf{R}_m(t)\mathbf{S}$ and consider the Lyapunov state transformation [17] $\mathbf{z}(t) = \mathbf{T}(t)\mathbf{x}(t)$, which preserves observability properties, where $\mathbf{T}(t) = \mathrm{diag}\left(\mathbf{I}_{n_{x_v}}, \mathbf{R}_m(t), \dots, \mathbf{R}_m(t) \right)$. It is a simple matter of computation to show that the new system dynamics are given by

$$\begin{cases} \dot{\mathbf{z}}(t) = \boldsymbol{\mathcal{A}}(t)\mathbf{z}(t) \\ \mathbf{y}(t) = \boldsymbol{\mathcal{C}}(t)\mathbf{z}(t) \end{cases},$$

where

$$\boldsymbol{\mathcal{A}}(t) = \begin{bmatrix} \mathbf{A}_v & \mathbf{0}_{n_{x_v} \times n_{x_m}} \\ \boldsymbol{\mathcal{A}}_{MV}(t) & \mathbf{0}_{n_{x_m} \times n_{x_m}} \end{bmatrix} \in \mathbb{R}^{(n_{x_v} + n_{x_m}) \times (n_{x_v} + n_{x_m})},$$

$$\boldsymbol{\mathcal{A}}_{MV}(t) = \begin{bmatrix} \boldsymbol{\mathcal{A}}_{MV_1}^T(t) & \dots & \boldsymbol{\mathcal{A}}_{MV_{n_{no}}}^T(t) \end{bmatrix}^T \in \mathbb{R}^{n_{x_m} \times n_{x_v}},$$

$$\boldsymbol{\mathcal{A}}_{MV_i}(t) = \begin{bmatrix} \mathbf{0}_{2 \times 1} & -\mathbf{R}_m(t) & \mathbf{0}_{2 \times 1} & \mathbf{R}_m(t)\mathbf{S}\,\mathbf{p}_{i_m}(t) \end{bmatrix},$$

and

$$\boldsymbol{\mathcal{C}}(t) = \begin{bmatrix} \mathbf{C}_z & \mathbf{0}_{1 \times n_{x_m}} \\ \mathbf{0}_{n_{x_m} \times n_{x_v}} & \mathrm{diag}\left(\mathbf{R}_m^T(t), \dots, \mathbf{R}_m^T(t) \right) \end{bmatrix},$$

$\boldsymbol{\mathcal{C}}(t) \in \mathbb{R}^{(1 + n_{x_m}) \times (n_{x_v} + n_{x_m})}$. The transition matrix associated with $\boldsymbol{\mathcal{A}}(t)$ is given by

$$\boldsymbol{\phi}(t, t_0) = \begin{bmatrix} \boldsymbol{\phi}_v(t, t_0) & \mathbf{0} \\ \boldsymbol{\phi}_{mv}(t, t_0) & \mathbf{I} \end{bmatrix},$$

where

$$\boldsymbol{\phi}_v(t, t_0) = \begin{bmatrix} 1 & \mathbf{0} & -(t - t_0) & 0 \\ \mathbf{0} & \mathbf{I} & \mathbf{0} & \mathbf{0} \\ 0 & \mathbf{0} & 1 & 0 \\ 0 & \mathbf{0} & 0 & 1 \end{bmatrix} \in \mathbb{R}^{n_{x_v} \times n_{x_v}}$$

and

$$\phi_{mv}(t, t_0) =$$
$$\begin{bmatrix} 0 & -\int_{t_0}^{t} \mathbf{R}_m(\sigma)d\sigma & \mathbf{0} & \int_{t_0}^{t} \mathbf{R}_m(\sigma)\mathbf{S}\mathbf{p}_{o_{1_m}}(\sigma)d\sigma \\ \vdots & \vdots & \vdots & \vdots \\ 0 & -\int_{t_0}^{t} \mathbf{R}_m(\sigma)d\sigma & \mathbf{0} & \int_{t_0}^{t} \mathbf{R}_m(\sigma)\mathbf{S}\mathbf{p}_{o_{n_{o_m}}}(\sigma)d\sigma \end{bmatrix}.$$

If $\mathcal{W}(t_0, t_f)$ denotes the observability Gramian associated with the pair $(\mathcal{A}(t), \mathcal{C}(t))$ on $[t_0, t_f]$ and $\mathbf{c} = \begin{bmatrix} c_1 & \mathbf{c}_2^T & c_3 & c_4 & \mathbf{c}_5^T & \dots & \mathbf{c}_{4+no}^T \end{bmatrix}^T$, it is a simple matter of computation to show that

$$\mathbf{c}^T \mathcal{W}(t_0, t_0 + \delta) \mathbf{c} = \int_{t_0}^{t_0+\delta} \|\mathbf{f}(\tau)\|^2 d\tau,$$

where

$$\mathbf{f}(\tau) :=$$
$$\begin{bmatrix} c_1 - c_3(\tau - t_0) \\ \mathbf{c}_5 - \int_{t_0}^{\tau} \mathbf{R}_m(\sigma)\mathbf{c}_2 d\sigma + \int_{t_0}^{\tau} \mathbf{R}_m(\sigma)\mathbf{S}\mathbf{p}_{o_{1_m}}(\sigma)c_4 d\sigma \\ \vdots \\ \mathbf{c}_{4+no} - \int_{t_0}^{\tau} \mathbf{R}_m(\sigma)\mathbf{c}_2 d\sigma + \int_{t_0}^{\tau} \mathbf{R}_m(\sigma)\mathbf{S}\mathbf{p}_{o_{n_{o_m}}}(\sigma)c_4 d\sigma \end{bmatrix}.$$

The first derivative of $\mathbf{f}(\tau)$ is given by

$$\frac{d}{d\tau}\mathbf{f}(\tau) := \begin{bmatrix} -c_3 \\ \mathbf{R}_m(\tau)(-\mathbf{c}_2 + \mathbf{S}\mathbf{p}_{o_{1_m}}(\tau)c_4) \\ \vdots \\ \mathbf{R}_m(\tau)(-\mathbf{c}_2 + \mathbf{S}\mathbf{p}_{o_{n_{o_m}}}(\tau)c_4) \end{bmatrix},$$

where, for the limit points t_0 and t_f, with a slight abuse of notation, this derivative is considered to be, respectively, the right and left derivatives of $\mathbf{f}$. Suppose now that the observability Gramian $\mathcal{W}(t_0, t_f)$ is not invertible. Then, there exists a unit vector $\mathbf{c}$ such that

$$\mathbf{c}^T \mathcal{W}(t_0, t_0 + t) \mathbf{c} = 0 \qquad (3)$$

for all $t \in \mathcal{T}$, which in turn implies that $\mathbf{f}(\tau) = \mathbf{0}$ and $\frac{d}{d\tau}\mathbf{f}(\tau) = \mathbf{0}$ for all $t \in \mathcal{T}$. In particular, for $t = t_0$, this immediately implies that $c_1 = 0$, $c_3 = 0$, and $\mathbf{c}_5 = \dots = \mathbf{c}_{4+no} = \mathbf{0}$. With that in mind, it is trivial to see that, under the conditions of the theorem, the only solution of $\frac{d}{d\tau}\mathbf{f}(\tau) = \mathbf{0}$ is $\mathbf{c}_2 = 0$ and $c_4 = 0$. But this contradicts the existence of a unit vector $\mathbf{c}$ such that (3) holds for all $t \in \mathcal{T}$. As such, the observability Gramian $\mathcal{W}(t_0, t_f)$ is invertible and, from [14, Lemma 1], the nonlinear system (2) is observable. ∎

Following the same approach of [14], the design of a filter with globally asymptotically stable error dynamics follows naturally with a Kalman filter, provided that the pair $(\mathbf{A}(t), \mathbf{C}(t))$ is uniformly completely observable. The following theorem addresses this issue.

Theorem 2: The pair $(\mathbf{A}(t), \mathbf{C}(t))$ is uniformly completely observable if there exists $\delta > 0$ such that, for all $\mathcal{T}_\delta = [t, t + \delta]$, with $t \geq t_0$, there exists $t_i \in \mathcal{T}_\delta$ for which there exist at least two observable landmarks, $\mathbf{p}_{o_{1_m}}(t_i)$ and $\mathbf{p}_{o_{2_m}}(t_i)$ satisfying $\mathbf{p}_{o_{1_m}}(t_i) \neq \mathbf{p}_{o_{2_m}}(t_i)$.

Proof: The proof follows similar steps to the proof of Theorem 1 but considering uniform bounds for all $t \geq t_0$ and intervals $[t, t + \delta]$. It is omitted due to the lack of space.

The reader is referred to [15] for a proof that follows similar steps, with slightly different system dynamics. ∎

Remark 1: It is important to stress that Theorem 1 and Theorem 2 provide only sufficient conditions. In fact, the nonlinear system (2) is observable in certain conditions even if a single landmark is available, if a certain persistent excitation condition is met, in line with what can be found in [15] for single vector observations. This more theoretical aspect of the problem will be addressed in future work.

IV. SLAM Filter Design

The design of the proposed sensor-based SLAM filter is presented in this section. In standard SLAM algorithms based on the Kalman filter, the vehicle position and orientation, as well as the position of any unobserved landmark, are propagated in open-loop, whereas in the proposed solution, only the unobserved landmarks are propagated in open-loop. It was shown in the previous section that the LTV system (2) is uniformly completely observable, under the conditions of Theorem 2. This is an important result that leads naturally to the design of a Kalman filter with globally asymptotically stable error dynamics. Without loss of generality and for simplicity of notation, let T_s denote the sampling period of the synchronized IMU, LASER scanner, and altitude sensors. Thus, considering that $\mathbf{x}_k := \mathbf{x}(t_k)$, with $t_k = kT_s + t_0$, $k \in \mathbb{N}_0$ and t_0 is the initial time, the Euler discretization of the system dynamics (2) with system disturbance and measurement noise yields

$$\begin{cases} \mathbf{x}_{k+1} = \mathbf{F}_k \mathbf{x}_k + \mathbf{w}_k \\ \mathbf{y}_{k+1} = \mathbf{H}_{k+1} \mathbf{x}_{k+1} + \mathbf{n}_{k+1} \end{cases}, \qquad (4)$$

where $\mathbf{F}_k = \mathbf{I}_{n_x} + T_s \mathbf{A}_k$, $\mathbf{H}_k = \mathbf{C}_k$, $\mathbf{w}_k \in \mathbb{R}^{n_x}$ and $\mathbf{n}_k \in \mathbb{R}^{n_y}$ are zero-mean discrete white Gaussian noise, with $E[\mathbf{w}_k \mathbf{w}_l^T] = \mathbf{Q}_k \delta_{k-l}$ and $E[\mathbf{n}_k \mathbf{n}_l^T] = \mathbf{R}_k \delta_{k-l}$, respectively, and δ_k denotes the Dirac delta function.

A. Prediction Step

The resulting discrete Kalman filter equations for the above system are standard [18]–[20]. Nonetheless, system (4) does not account for the unobserved landmarks $\mathbf{x}_{MU}$, which have to be propagated in open-loop using the nonlinear equations defined in (1). Using the full system state vector $\mathbf{x}_F = \begin{bmatrix} \mathbf{x}^T & \mathbf{x}_{MU}^T \end{bmatrix}^T$, the complete prediction equations are given by

$$\begin{cases} \hat{\mathbf{x}}_{F_{k+1|k}} = \mathbf{F}_{F_{k|k}} \hat{\mathbf{x}}_{F_{k|k}} \\ \mathbf{P}_{F_{k+1|k}} = \mathbf{F}_{F_{k|k}} \mathbf{P}_{F_{k|k}} \mathbf{F}_{F_{k|k}}^T + \mathbf{Q}_{F_k} \end{cases},$$

where $\hat{\mathbf{x}}_F$ denotes the estimated state vector and $\mathbf{P}_F$ the state covariance matrix, the disturbance matrix is defined as $\mathbf{Q}_F = \text{diag}(\mathbf{Q}, \mathbf{Q}_{MU})$, whereas the covariance matrix can be decomposed as in observable, unobservable, and crossed terms. The full transition matrix $\mathbf{F}_{F_{k|k}}$ is defined as

$$\mathbf{F}_{F_{k|k}} = \begin{bmatrix} \mathbf{F}_k & \mathbf{0}_{n_x \times n_{xMU}} \\ \mathbf{F}_{UO_{k|k}} & \mathbf{F}_{MU_{k|k}} \end{bmatrix},$$

where the remaining undefined terms can be easily inferred from the nominal system dynamics (1).

B. Update Step

At each sampling instant a new altitude measurement and a new LASER horizontal profile are obtained and projected into the horizontal frame $\{H\}$. The projected altitude measurement is readily used in the filter, whereas the LASER profile is fed to a landmark detection algorithm, and the observed landmarks are associated with the existing state landmarks using the joint compatibility branch and bound (JCBB) algorithm [21]. Having obtained the new association pairs between measured landmarks and existing state landmarks, the sets of observed and unobserved landmarks, respectively, $\mathcal{I}_O$ and $\mathcal{I}_U$, and the observable and unobservable state vectors are redefined. In addition, the association algorithm naturally provides the innovation vector, $\boldsymbol{\nu}_{k+1} = \mathbf{y}_{k+1} - \mathbf{H}_{k+1}\,\hat{\mathbf{x}}_{k+1|k}$, and the respective covariance matrix, $\mathbf{S}_{k+1} = \mathbf{H}_{k+1}\,\mathbf{P}_{k+1|k}\,\mathbf{H}_{k+1}^T + \mathbf{R}_{k+1}$. Thus, for the update step all the filter estimates related with the unobserved landmarks remain unchanged, that is, $\hat{\mathbf{x}}_{MU_{k+1|k+1}} = \hat{\mathbf{x}}_{MU_{k+1|k}}$, $\mathbf{P}_{MU_{k+1|k+1}} = \mathbf{P}_{MU_{k+1|k}}$, and also $\mathbf{P}_{UO_{k+1|k+1}} = \mathbf{P}_{UO_{k+1|k}}$, whereas for the observed state, is just a matter of using the standard discrete Kalman filter update equations.

V. EXPERIMENTAL RESULTS

This section describes the experimental setup and presents the results for the sensor-based SLAM filter introduced before. To validate the convergence properties and the consistency of the proposed algorithm, an instrumented quadrotor was hand-driven along a path of about 60 meters in an indoor environment with a loop, as shown below in Fig. 3, at an average speed of 0.4 m/s. The trajectory described by the vehicle starts near the bottom right corner and circulates counter clockwise until some of the first landmarks detected are once again visible. The vehicle is a customized quadrotor UAV, property of ISR, equipped with a MEMSENS nanoIMU, a Maxbotix XL SONAR for altitude measurement, and a Hokuyo UTM-30LX LASER scanning device mounted horizontally to provide horizontal profiles of the surroundings. The disturbance covariance matrix, assumed Gaussian, for the vehicle dependent state variables is defined as $\mathbf{Q}_V = T_s \operatorname{diag}\left(\sigma_z^2, \sigma_v^2 \mathbf{I}_3, \sigma_{b_r}^2\right)$, with $\sigma_z = 0.04$ m, $\sigma_v = 0.02$ m/s, $\sigma_{b_r} = 5.7 \times 10^{-5}$ deg/s, and the landmark position disturbance covariance matrix is given by $\mathbf{Q}_{\mathbf{P}_i} = T_s \sigma_p^2 \mathbf{I}_2$, $\sigma_p = 0.07$ m. The altitude measurement is also considered to be zero-mean Gaussian distributed noise with variance $\mathbf{R}_z = \sigma_z^2$, $\sigma_z = 0.03$ m, and the landmark position measurement noise covariance matrix is given as a function of the angular and range standard deviation values, $\sigma_\alpha = 3.75$ deg, $\sigma_{\rho_1} = 0.15$ m, and $\sigma_{\rho_2} = 0.25$ m, assuming a small angle approximation (see [12] for more details).

When analyzing the convergence properties of any navigation filter, the main goal is to observe a decreasing uncertainty in all variables. This can readily be seen in Fig. 1, where the uncertainty of all the vehicle related variables decreases over time. Furthermore, it can be seen that the uncertainty of each landmark decreases whenever it is observed and increases otherwise, as shown in Fig. 2.
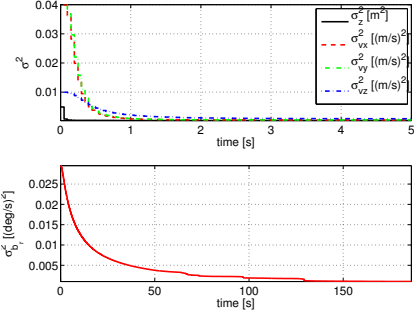

Fig. 1. Uncertainty of vehicle related variables: altitude, linear velocity, and gyro rate bias.
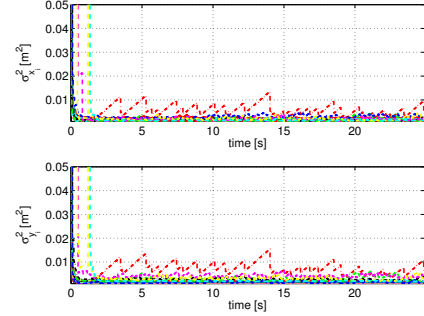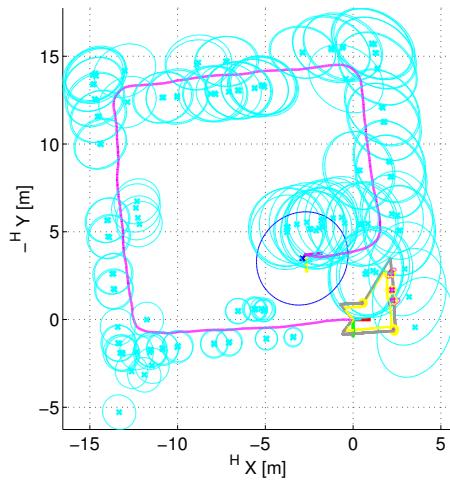

Fig. 2. Uncertainty of landmark position, showing the detailed evolution of the position variance for the first 20 observed landmarks, where each line represents a landmark.
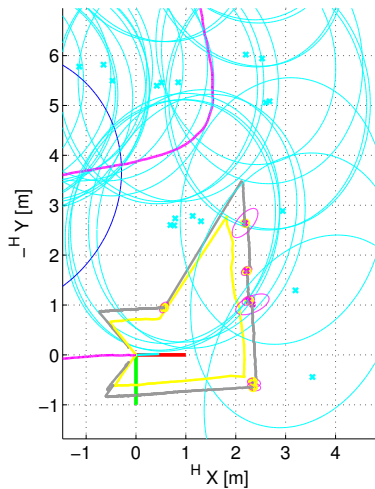
In sensor-based SLAM, the localization is trivial, as the vehicle is at the origin and aligned with the body frame. As for the mapping, the algorithm provides at each instant a map of the environment with consistent uncertainty estimates. These results are presented in Fig. 3, with a detailed view of the last part of the trajectory (lower right corner of the map) in Fig. 3(b). It can be seen that in this sensor-based framework, as there is no vehicle localization uncertainty, the unobserved landmarks uncertainty increases allowing for a consistent map building, and eventually to close a loop. The uncertainty of the older landmarks at the bottom right corner, which are deliberately left as duplicates of the new landmarks being detected, would enable the proper association and loop closing procedure for the global sensor-based map. A more thorough presentation of these results is found in the companion paper [12].

VI. CONCLUSIONS AND FUTURE WORK

This paper presents the problem formulation, analysis, design, and experimental performance evaluation of a globally asymptotically stable sensor-based SLAM filter. Conversely to traditional EKF-SLAM algorithms, the proposed method avoids the attitude representation of the vehicle in the filter state, enabling the modification of the nominal nonlinear dynamics into a structure that can be regarded as LTV for analysis and filter design. The filter does not rely on any odometry sensor, but rather on angular rate measurements, having the byproduct of estimating the linear velocity in the vehicle frame, as well as the rate gyro bias and the

(a) Complete map

(b) Detailed view

Fig. 3. Map and trajectory in $\{H\}$ frame, featuring the landmark position and 95% confidence bounds, depicted in light blue, and the trajectory of the vehicle, in magenta. The duplicate landmarks, that could be used for loop closure are also depicted in magenta, whereas the current laser profile is depicted in gray and the visibility polygon in yellow.

altitude. In the second part of this work, presented in the companion paper [12], the vehicle attitude, position, and the estimated environment map described in inertial frame are computed resorting to the closed form solution of an optimization problem. The performance and consistency of the proposed solution to the SLAM problem is validated in a structured real world environment, where the algorithm shows the reduction of the uncertainty in every state variable but the unobserved landmarks, and produces a consistent map estimation that can be used to close a 60 meter long loop.

Future work includes the implementation of a loop closure method and the real time optimized implementation and testing of the algorithm in UAVs. In addition, the authors plan to compare the performance and consistency of the proposed sensor-based SLAM algorithm with the state-of-the-art SLAM algorithms.

REFERENCES

[1] R. C. Smith and P. Cheeseman, "On the Representation and Estimation of Spatial Uncertainty," *International Journal of Robotics Research*, vol. 5, no. 4, pp. 56–68, 1986.

[2] H. Durrant-Whyte, "Uncertain geometry in robotics," *IEEE Journal of Robotics and Automation*, vol. 4, no. 1, pp. 23–31, feb 1988.

[3] H. Durrant-Whyte and T. Bailey, "Simultaneous Localization and Mapping: part I," *Robotics Automation Magazine, IEEE*, vol. 13, no. 2, pp. 99–110, 2006.

[4] T. Bailey and H. Durrant-Whyte, "Simultaneous Localization and Mapping (SLAM): part II," *Robotics Automation Magazine, IEEE*, vol. 13, no. 3, pp. 108–117, 2006.

[5] G. Dissanayake, P. Newman, H. Durrant-Whyte, S. Clark, and M. Csobra, "A solution to the simultaneous localisation and mapping (SLAM) problem," *IEEE Transactions on Robotics and Automation*, vol. 17, no. 3, pp. 229–241, 2001.

[6] S. Huang and G. Dissanayake, "Convergence and Consistency Analysis for Extended Kalman Filter Based SLAM," *IEEE Transactions on Robotics*, vol. 23, no. 5, pp. 1036–1049, oct. 2007.

[7] S. J. Julier and J. K. Uhlmann, "A counter example for the theory of simultaneous localization and map building," in *Proceedings of the 2001 IEEE International Conference on Robotics and Automation*, May 2001, pp. 4238–4243.

[8] T. Bailey, J. Nieto, J. Guivant, M. Stevens, and E. Nebot, "Consistency of the EKF-SLAM algorithm," in *Proceedings of the 2006 IEEE/RSJ International Conf. Intell. Robots Syst.*, October 2006, pp. 3562–3568.

[9] J. Castellanos, J. Neira, and J. Tardós, "Limits to the consistency of EKF-based SLAM," in *Proceedings of the 5th IFAC Symposium on Intelligent Autonomous Vehicles*, July 2004.

[10] J. A. Castellanos, R. Martinez-Cantin, J. D. Tardós, and J. Neira, "Robocentric Map Joining: Improving the Consistency of EKF-SLAM," *Robotics and Autonomous Systems*, vol. 55, no. 1, pp. 21–29, January 2007.

[11] G. Huang, A. Mourikis, and S. Roumeliotis, "A First-Estimates Jacobian EKF for Improving SLAM Consistency," in *Experimental Robotics*, ser. Springer Tracts in Advanced Robotics, O. Khatib, V. Kumar, and G. Pappas, Eds. Springer Berlin Heidelberg, 2009, vol. 54, pp. 373–382.

[12] B. J. Guerreiro, P. Batista, C. Silvestre, and P. Oliveira, "Sensor-based Simultaneous Localization and Mapping – Part II: Online Inertial Map and Trajectory Estimation," in *Proceedings of the 2012 American Control Conference*, June 2012.

[13] P. Batista, C. Silvestre, and P. Oliveira, "Optimal Position and Velocity Navigation Filters for Autonomous Vehicles," *Elsevier Automatica*, vol. 46, no. 4, pp. 767–774, April 2010.

[14] ——, "Single Range Aided Navigation and Source Localization: observability and filter design," *Systems & Control Letters*, vol. 60, no. 8, pp. 665–673, Aug. 2011.

[15] ——, "Sensor-based Globally Asymptotically Stable Filters for Attitude Estimation: Analysis, Design, and Performance Evaluation," *IEEE Transactions on Automatic Control*, July 2011, accepted for publication.

[16] ——, "Partial attitude and rate gyro bias estimation: observability analysis, filter design, and performance evaluation," *International Journal of Control*, vol. 84, no. 5, pp. 895–903, May 2011.

[17] R. Brockett, *Finite Dimensional Linear Systems*. Wiley, 1970.

[18] R. Kalman and R. Bucy, "New Results in Linear Filtering and Prediction Theory," *Transactions of the ASME - Journal of Basic Engineering*, vol. 83, no. 3, pp. 95–108, March 1961.

[19] A. Gelb, *Applied Optimal Estimation*. MIT Press, May 1974.

[20] A. Jazwinski, *Stochastic Processes and Filtering Theory*. Academic Press, Inc., 1970.

[21] J. Neira and J. Tardós, "Data Association in Stochastic Mapping Using the Joint Compatibility Test," *IEEE Transactions on Robotics and Automation*, vol. 17, no. 6, pp. 890–897, December 2001.